

COMPARATIVE STUDY OF THE SATURN'S RINGS WITH ATMOSPHERELESS SOLAR SYSTEM SATELLITES USING HAPKE PHOTOMETRIC PARAMETERS E. Déau¹, A. Brahic², S. Charnoz³ and C. C. Porco⁴, ¹CEA Service d'Astrophysique AIM, bâtiment 709, Orme des Merisiers 91191 Gif-sur-Yvette, France edeau@cea.fr, ^{2,3}Université Paris 7 AIM, bâtiment Condorcet 10 rue A. Domon et L. Duquet, 75205 Paris Cedex 13 France, brahic@cea.fr, charnoz@cea.fr, ⁴CICLOPS, 3100 Walnut Street, Suite A535, Boulder COLORADO 80303, USA, carolyn@ciclops.org



Fig. 1: Natural color views of the Saturn's rings: C ring, B ring, Cassini Division and A ring (from left to right, with increasing distance from Saturn's center) at different phase angles ($\alpha=70^\circ$ at top and $\alpha=150^\circ$ at bottom) obtained with the ISS/Cassini images

Introduction: From July 2004 to now, ISS cameras of the Cassini spacecraft observed the Saturn System with an unprecedented radial resolution and phase angle coverage (figure 1). We obtained from a dataset of 150 images in broadband CLEAR filters ($\lambda=611\pm 450$ nm) 211 phase functions spanning from 0.01° to 179° of phase angle in various locations in the Saturn's main rings (1 pixel ~ 50 km). This is the first time that phase functions of the Saturn's rings cover backscattering and forward scattering directions. In a first step, we have fitted the phase functions with the Hapke model [1] which is the photometric model mostly used in the community, see [2-4] for a review, although this model has several important physical weaknesses [5,6]. With the photometric parameters obtained by fitting such a model to the ISS/Cassini data, we compared our results with the previously published Hapke parameters derived by the photometric community on various phase curves of the Solar System satellites.

Data processing: The Hapke model uses 6 free parameters for the Henyey-Greenstein 2-terms' form ($b, c, \omega_0, \theta, h, B_0$) or 7 free parameters for the Henyey-Greenstein 3-terms' form ($g_1, g_2, f, \omega_0, \theta, h, B_0$). Our phase functions were geometrically corrected by the Chandrasekhar inversion [7] and fitted by using a chi-square minimization in the space parameters. In general, our phase functions were better fitted with the Henyey-Greenstein 3-terms' form.

Results and discussion: Here, we focus only on 4 Hapke parameters which present the strongest dependencies with the single scattering albedo ω_0 : (i) the asymmetry parameter $g=f g_1+(1-f) g_2$ in figure 2, (ii) the macroscopic roughness θ in figure 3, (iii) the Shadow hiding amplitude B_0 in figure 4, (iv) the Shadow hiding angular width h in figure 5. First of all, we noticed that the range's albedo of Saturn's rings is wider than those of all satellites joined together. We superimposed data points of these planetary objects (without distinction), by considering the reviews on Hapke parameters of [3,4].

Anisotropy of the single scattering. Figure 2 shows that the Saturn's rings can be both backscatters (with $g < 0$) and forward-scatters (with $g > 0$), for a minority of A and C rings and Cassini Division regions). Since a long time, planetary objects had invariably negative values of g [8], except terrestrial snowbanks [9]. Our study demonstrates that positive values of g can be obtained with the Hapke model, if phase curves exhibit strong forward-scattering peak at $\alpha > 170^\circ$.

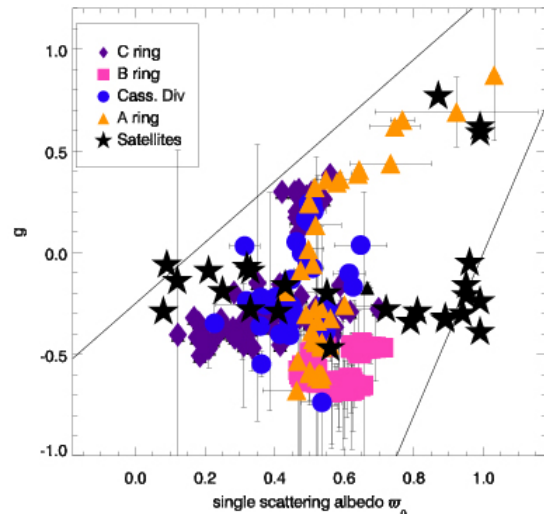


Fig.2. Variation of the asymmetry parameter g of Hapke model [1] with the single scattering albedo ω_0 . Solid lines are empirical functions to the data boundaries (as for figures 3, 4 and 5).

Macroscopic roughness. Figure 3 shows that the Saturn's rings are substantially rougher than the satellites. However, the linear fit to the data shows that their general behaviors are quite the same. Indeed, we found in both cases an increase of θ with increasing ω_0 . If the macroscopic roughness represents the roughness of one particle, the tendency of $\theta=f(\omega_0)$ can be simply explained in the case of the Saturn's rings. Indeed, recent modeling supports the idea that particles in smaller optical depth regions are significantly smoother: this could be due to the dominance of collisional compaction over transient clustering [10]. In contrast, in high

optical depth regime, particles are aggregates [11-13]. Because the single scattering albedo ω_0 is positively correlated with the optical depth τ of the Saturn's rings [3, 14], the trend of $\theta=f(\omega_0)$ is then confirmed by dynamical arguments. However, it's complicated to explain why the Saturn's rings are rougher than the satellites and why the satellites' roughness increases with increasing albedo ω_0 .

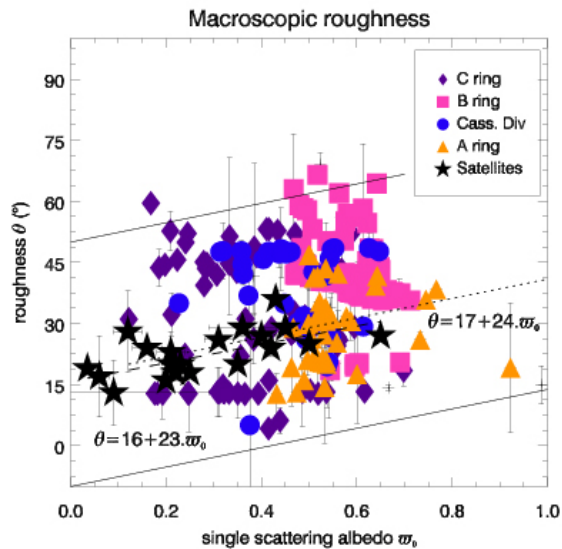


Fig.3. Variation of the macroscopic roughness of Hapke model [1] with the single scattering albedo ω_0 . Dashed and dotted lines correspond to a linear fit to the data for rings and satellites respectively with a correlation coefficient of 65% and 24%.

Amplitude and slope of the Shadow hiding. In figure 4, are plotted the shadow hiding amplitudes $B_0=f(\omega_0P(0^\circ))$ in the Log-Log representation of [2]. Interestingly, the correlation found by [2] fits well our data points; however Saturn's rings have systematically smaller value of B_0 . This is due to the fact that our phase functions cover the opposition ($\alpha>0.01^\circ$) whereas in for B_0 compiled by [2], the opposition surge is missing because the phase function starts from a few degrees. Moreover, for the Saturn's rings we found that $B_0<1$ in a majority of cases whereas in [2] $B_0>1$, which is strictly forbidden by the model [1]. The extrapolation of missing data may be responsible for B_0 values greater than unity.

In recent numerical simulations of the shadow hiding [15], the amplitude of the peak and the absolute slope of the linear part increase with increasing optical depth τ , table 1 (or increasing ω_0 because ω_0 and τ are correlated [3, 14]).

Tab.1. Variations of the amplitude of the surge and the absolute slope S of the linear part computed with numerical simulations of shadow hiding of [15].

Optical depth τ	0.1	0.2	0.3	0.4	0.54
$A=I(0^\circ)/I(5^\circ)$	1.001	1.009	1.015	1.030	1.039
$S= I(5^\circ)-I(30^\circ)/25^\circ$	0.001	0.002	0.005	0.007	0.008

The slope's trend was confirmed by morphological studies on the phase function of the Saturn's rings [16], the Solar System satellites [17] and Solar System asteroids [18]. Indeed, [16, 17] lead to an increase of S (in $\omega_0P.\text{deg}^{-1}$ and $I/F.\text{deg}^{-1}$) with τ and ω_0 , [18] to a decrease of β (in $\text{mag}.\text{deg}^{-1}$) with albedo, which is also an increase of β (in $I/F.\text{deg}^{-1}$) with albedo. However, the shadow hiding amplitude B_0 is defined as a decreasing function of albedo [1] and thus contradicts predictions of [15]. In figure 5 we have represented an absolute slope $S=f(\omega_0)$, where S uses 3 Hapke parameters (B_0 , h and $\omega_0P(0^\circ)$). We obtained a slight increase of S with increasing albedo. This is clearly the proof that Hapke model agrees with numerical simulations. A possible explanation of the decrease of B_0 with increasing ω_0 is that B_0 is not the amplitude of the shadow hiding but the full amplitude of the opposition surge. In this way, variations of $B_0=f(\omega_0)$ agree with the trend of the morphological surge amplitude [16, 17].

Conclusion: This comparative study of the Hapke parameters between the Saturn's rings and the Solar System satellites shows common dependencies with albedo ω_0 . We demonstrate that the asymmetry parameter g , the macroscopic roughness and the slope of the shadow hiding increase all with increasing albedo ω_0 , which is common for the Saturn's rings and the Solar System satellites.

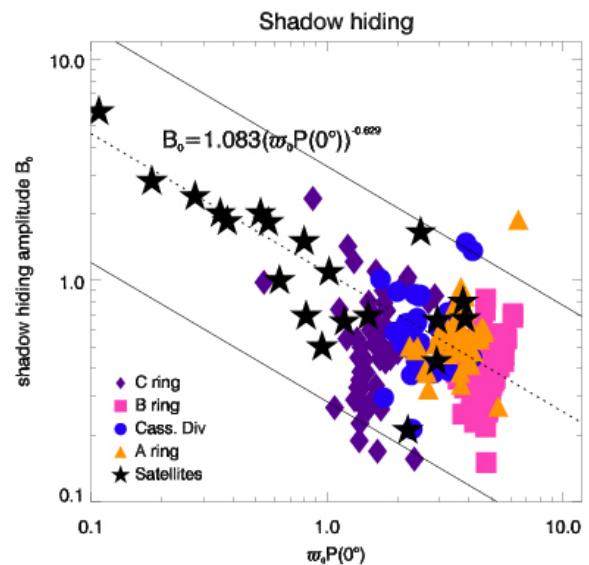


Fig.4. Variation of the shadow hiding amplitude B_0 of Hapke model [1] with the phase function at opposition $\omega_0P(0^\circ)$. The dotted line corresponds to an empirical fit of [2] with a correlation coefficient of 92%.

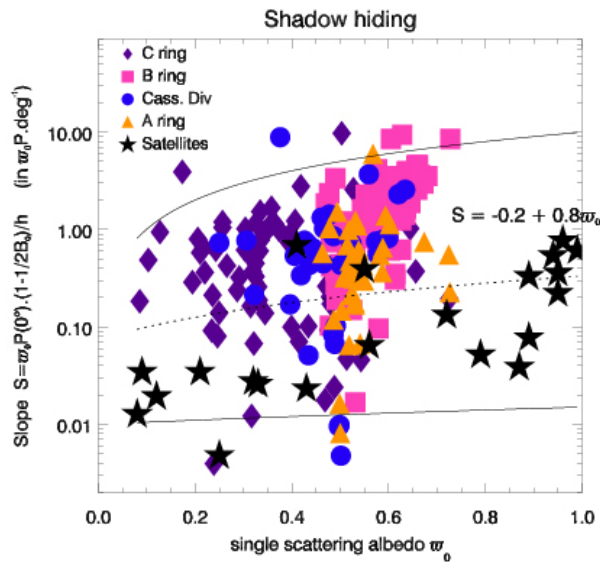


Fig.5. Variation of the shadow hiding slope S computed with B_0 , h and $\omega_0 P(0^\circ)$ of Hapke model [1]. The dotted line corresponds to a linear fit to the Solar System satellites data points with a correlation coefficient of 24%.

References: [1] Hapke B. (1986) *Icarus*, 67, 264-280. [2] Helfenstein P. et al. (1997) *Icarus*, 128, 2-14. [3] Déau E. (2007) PhD Thesis Université Paris7. [4] Cord A. M. et al. (2003) *Icarus*, 165, 414-427. [5] Shepard M. K., and Helfenstein P. (2007) *JGR*, 112, E03001. [6] Shkuratov Yu. et al. (2007) *JQSRT*, 106, 487-508. [7] Chandrasekhar S. (1960) New York, Dover. [8] Cuzzi J. N. and Estrada P. R. (1998) *Icarus*, 132, 1-35. [9] Verbiscer A. J and Veverka J. (1990) *Icarus*, 88, 418-428. [10] Poulet F. et al. (2002) *Icarus*, 158, 224-248. [11] Weidenschilling S. J. et al. (1984) In Planetary Rings (R Greenberg and A. Brahic, Eds) 367-416. [12] Salo H. (1992) *Icarus*, 96, 85-106. [13] Richardson D. C. (1994) *MNRAS*, 269, 493-511. [14] Doyle L. R. et al. (1989) *Icarus*, 80, 104-135. [15] Stankevich D. G. et al. (1999) *JQSRT*, 63, 445-448. [16] Déau E. et al. (2006) *BAAS* 38, Abstract#51.01. [17] Déau E. et al. (2008) *LPSC XXXIX*, Abstract#1391. [18] Belskaya I. N. and Shevchenko V. G. (2000) *Icarus*, 147, 94-105